Food and Public Health 2016, 6(1): 1-7
DOI: 10.5923/j.fph.20160601.01

Modeling and Optimization of Supercritical Fluid Extraction of Compounds from *Campomanesia xanthocarpa* Fruits: Comparison between Artificial and Diffusion Based Models

Neshat Rahimpur[1], Tahmasb Hatami[2], M. Angela A. Meireles[2,*]

[1]Department of Chemical Engineering, Faculty of Engineering, University of Kurdistan, Sanandaj, Iran
[2]LASEFI/DEA/FEA (School of Food Engineering), UNICAMP (University of Campinas), Campinas, Brazil

Abstract The extracts of *Campomanesia xanthocarpa* fruits and leaves have many reported applications, especially in folk medicine for the treatment of several diseases. As it is hard to experimentally investigate the influences of the operating conditions on the supercritical fluid extraction (SFE) yield in a continuous range, modeling of this process can be an efficient method for this purpose. In this paper, the potential of two models, namely artificial neural network (ANN) and Hot Sphere Diffusion (HSD), were examined to simulate the SFE of compounds from *Campomanesia xanthocarpa* fruits. Noticeably, the numbers of adjustable variables were approximately the same for both models: 10 for the HSD model compared to 11 for the ANN model. A comparison of the models with experimental data points indicated the superiority of the ANN model over the HSD model. After verification of the ANN model, the influence of pressure and temperature on the extraction yield was studied, and the optimum temperature and pressure for maximizing the extraction yield were determined. The influence of operating conditions at low extraction times was slightly complicated, but for higher extraction durations, increasing the pressure and temperature had respectively a positive and negative effect on the extraction yield.

Keywords Supercritical extraction, Simulation, Sensitivity analysis

1. Introduction

Campomanesia xanthocarpa is a type of tree that can be found in Brazil, Paraguay, Argentina, and Uruguay [1]. The extracts obtained from the fruits of this tree have many applications, such as in food and medicine industries for the treatment of gastric ulceration, overweight patients, and diabetes mellitus [2-5]. Several extraction techniques have been used for obtaining extracts from this fruit, and SFE has proved to be the most efficient method [6]. Czaikoski et al. studied the SFE of compounds from *Campomanesia xanthocarpa* fruits at pressures of 15.0, 20.0, and 25.0 MPa and temperatures of 313.15, 333.15, and 353.15 K [6]. Gas chromatography analysis showed that the obtained extracts under various temperatures and pressures had similar chemical compositions of α-eudesmol, β-eudesmol, γ-eudesmol, caryophyllene (E), α-sabinene, β- sabinene, germacrene B, δ-cadinene, humulene and selina-3, 7(11)-diene [6].

* Corresponding author:
maameireles@gmail.com (M. Angela A. Meireles)
Published online at http://journal.sapub.org/fph

Because there are many factors that influence the SFE efficiency, it is often difficult to examine this process using only pure experimental data. Mathematical models can be very helpful to investigate this complex process perfectly.

Many different types of diffusion based models have been developed over the years to predict the SFE from various seeds [7-9]. The main advantage of these models is that they are completely understandable from an engineering point of view as they are based on the mass conservation law. These models, however, are not appropriate for the cases in which accuracy is very important. Moreover, mathematical modeling of the SFE process is not always possible as these models usually require an excessive number of parameters, such as the critical properties of the extract, the porosity of particles, the void fraction of extractor, and the internal and external mass transfer coefficients. One of the most popular models that can be employed for such complicated processes is ANN. The structure of this famous model was originally inspired by the organization of the human brain [10]. Due to the development of modern computational methods, ANN has increasingly become an interesting approach for the modeling of complex systems without the requirement to

understand the nature of the involved processes. This powerful technique has been used by many researchers for the modeling of various chemical processes. For example, Izadifar and Abdolahi [11] applied an ANN model together with a mass-transfer based mathematical model to simulate the SFE of compounds from black pepper. Their model contained five input variables: extraction time, particle size, pressure, temperature, and supercritical carbon dioxide mass flow per unit mass of solid. It was revealed that the ANN model was more accurate than the mass-transfer based model. In particular, the regression coefficient of more than 0.96 indicated an excellent agreement between ANN prediction and experimental SFE data. In another relevant research study, Kuvendziev et. al [12] provided an efficient ANN model to simulate the extraction from lyophilized viscera matrices. The proposed ANN model, which had four inputs, one output, and three layers, fitted successfully the experimental data, with a regression coefficient of well over 0.99. Additional applications of ANN in SFE can be found in the papers presented by Ghoreishi and Heidari [13], Kamali and Mousavi [14], and Khajeh et. al [15].

The present paper describes the modeling of SFE from *Campomanesia xanthocarpa* fruits using both ANN and HSD models using literature data [6]. The predictability of both models was compared in terms of the extraction yield using experimental data. Using the developed models, this paper also described the general trend of SFE yield, even for operating conditions that were not measured experimentally. To the best of our knowledge, the ANN and mathematical modeling of SFE from *Campomanesia xanthocarpa* fruits has not been reported so far in the literature.

2. Materials and Methods

This paper is divided into two distinct parts. The first part describes the experimental data together with two applied models. The second part includes evaluation of the models and optimization of the process in term of SFE performance.

2.1. Experimental Data Points

All data of the current study were taken from a paper presented by Czaikoski et. al [6]. They reported 90 data points involving the SFE yield of *Campomanesia xanthocarpa* fruits as functions of temperature, pressure, and extraction time [6]. Note that both applied models contained 3 inputs, namely, temperature, pressure, and extraction time, and only one output, namely, extraction yield; the ranges of experimental data were 313.15 to 353.15 K for temperature, 15 to 25 MPa for pressure, 0 to 170 min for extraction time, and 0 to 3.76 g extract per 100 g of particles for extraction yield.

2.2. Applied Models

2.2.1. ANN Model

ANN has been widely used for modeling as it is able to learn quite complicated systems [16-19]. ANN contains several layers together with some simple units in each layer called neurons. ANN architectures have one input layer, one or several hidden layers, and one output layer. Each neuron in the hidden and output layers is attached to some constants, called weights and bias, and some transfer functions. Despite the capability of ANN for constructing a precise model, it is difficult to understand the physical meaning of its parameters. Thus, ANN models are usually referred to as black-box models. However, several techniques have been provided in literature to illuminate the ANN parameters and identify their impact on the model performance [20]. For constructing ANN model in this paper, the whole experimental dataset was separated randomly into three distinct parts: 40% of the data were used for model training, called the training set, 30% of them were used for model evaluation, called the test set, and the remaining 30% were employed to address the overtraining, known as the validation set.

2.2.2. HSD Model

The HSD model is based on several simplifying assumptions: (1) the extractor involves spherical single-size particles; (2) the gradients of velocity, pressure, temperature, and solute concentration within the fluid are neglected; (3) different solutes in the extract are considered as single compound; (4) sample shrinkage is neglected; (5) the diffusion coefficient of extract through the particles is constant. Using these assumptions and based on the second Fick's law, the mass balance across a particle in the extractor can be written as follows [21]:

$$\frac{\partial C}{\partial t} = \frac{D_e}{r^2}\frac{\partial}{\partial r}\left(r^2\frac{\partial C}{\partial r}\right) \quad (1)$$

Where C is the solute concentration in the particle, r is the distance from the particle center, and D_e is the diffusion coefficient. In fact, Fick's second law explains how the concentration changes with time. The boundary and initial conditions are:

$$at\ r = 0, t > 0 \implies C = finite \quad (2)$$

$$at\ r = R, t > 0 \implies C = C^* \quad (3)$$

$$at\ t = 0, 0 < r < R \implies C = C_0 \quad (4)$$

Where C_0 and C^* are the initial and equilibrium solute concentration in the particle, respectively. An analytical solution of equation (1) is given by [21]:

$$\frac{C-C_0}{C^*-C_0} = 1 + \frac{2R}{\pi r}\sum_{n=1}^{\infty}\frac{(-1)^n}{n}\sin\left(\frac{n\pi r}{R}\right)exp\left(-\left(\frac{n\pi}{R}\right)^2 D_e t\right) \quad (5)$$

Consequently, it can be proved that the extraction yield is given by the following equation [21]:

$$\frac{m_t}{m_F} = \frac{m_\infty}{m_F}\left(1 - \frac{6}{\pi^2}\sum_{n=1}^{\infty}\frac{1}{n^2}exp\left(-\left(\frac{n\pi}{R}\right)^2 D_e t\right)\right) \quad (6)$$

Where m_F is the total mass of feed, m_t denotes the total mass of extract at a given time t, and m_∞ symbolizes the corresponding quantity at infinite time. It should be noted that $\frac{m_\infty}{m_F}$ and D_e are the two adjustable parameters of this model.

2.3. Statistical Parameter for Evaluation of the Models

To test the statistical success of the models, mean square error (MSE) was used. This well-known statistical parameter is defined using the following correlation:

$$MSE = \frac{1}{N}\sum_{i=1}^{N}\left(\left(\frac{m_t}{m_F}\right)_i^{model} - \left(\frac{m_t}{m_F}\right)_i^{exp}\right)^2 \quad (7)$$

Where $\left(\frac{m_t}{m_F}\right)_i^{exp}$ is the experimental extraction yield of the ith data, and $\left(\frac{m_t}{m_F}\right)_i^{model}$ is the corresponding model value. The smaller the MSE, the higher the prediction ability of the model would be.

3. Results and Discussion

3.1. Evaluation of the Models

For ANN modeling, a comprehensive search for obtaining an ANN architecture with high forecast ability was employed. The model parameters were determined such that the ANN model approximated the experimental data points. According to the authors' experiences, an ANN model with one hidden layer could be a satisfactory model. However, determining the number of neurons in the hidden layer is not a simple task. In this study, a trial-and-error procedure was considered for determining the adequate number of neurons. For this purpose, the number of neurons was changed from 1 to 5. Next, the best ANN architecture to achieve the minimum MSE value was determined for each number of neurons. Figure 1 illustrates the trend of the MSE in terms of the number of neurons. Initially, an obvious reduction of the deviation is observed between the ANN model and the experimental data, in terms of the MSE. The MSE decreased dramatically from just under 0.11 for one neuron to just over zero for two neurons. This decline in the MSE is quite natural because a higher number of neurons correspond to a higher number of adjustable parameters. However, the MSE, as shown in this figure, remained approximately unchanged with application of more than two neurons in the hidden layer. Thus, two neurons were regarded as the optimum neuron number for constructing the ANN model.

Regarding the HSD model, its adjustable parameters were determined so that the difference between the model and experimental data, in terms of MSE, was minimized. Genetic algorithm optimization technique [22-25] was employed for this purpose. The adjustable parameters for both ANN and HSD models are presented in Table 1. In Table 1, iw_{mn} indices the weight from the nth input element to the mth neuron of the hidden layer, lw_i is the weight from the ith neuron activation function of the hidden layer to the output neuron, b_i is the bias of ith neuron, f^1 is the activation function of all neurons in the hidden layer, and f^2 is the activation function of output layer.

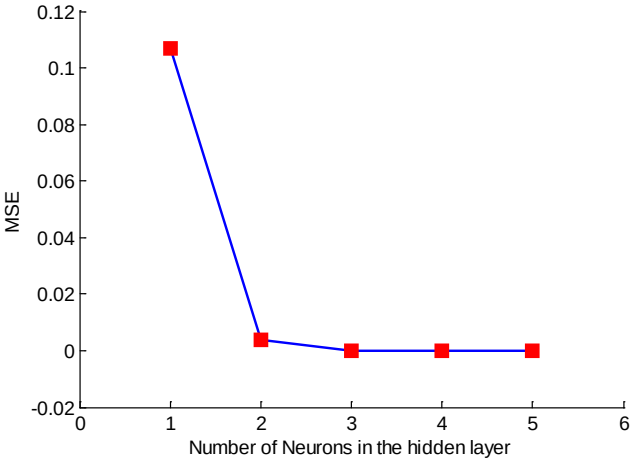

Figure 1. The influence of the number of neurons in the hidden layer on the deviation between the ANN model and the experimental data

Table 1. The numerical values of the weights and biases and the activation functions of the ANN models as well as the adjustable parameters of the HSD model

ANN Model		HSD Model		
	Value	**Run**	**$m_\infty/m_F \times 100$**	**D_e (m^2/s)**
iw_{11}	-6.6186	Exp. 1	0.9	9.97^{-13}
iw_{21}	0.3611	Exp. 2	4.0	1.73^{-13}
iw_{12}	7.266	Exp. 3	3.0	5.31^{-13}
iw_{22}	-0.6143	Exp. 4	8.3	7.53^{-14}
iw_{13}	0.4872	Exp. 5	8.9	9.40^{-14}
iw_{23}	1.4075	-	-	-
lw_1	1.7095	-	-	-
lw_2	5.6921	-	-	-
b_1	-0.1057	-	-	-
b_2	2.8469	-	-	-
b_3	-6.2044	-	-	-
f^1	Logsig	-	-	-
f^2	Purelin	-	-	-

To evaluate the predictability of both models, comparisons between the models and the experimental data are illustrated in Figures 2 and 3. Clearly, the HSD model is not so accurate in Figure 2, whereas the ANN model passes precisely through the experimental data points (Figure 3).

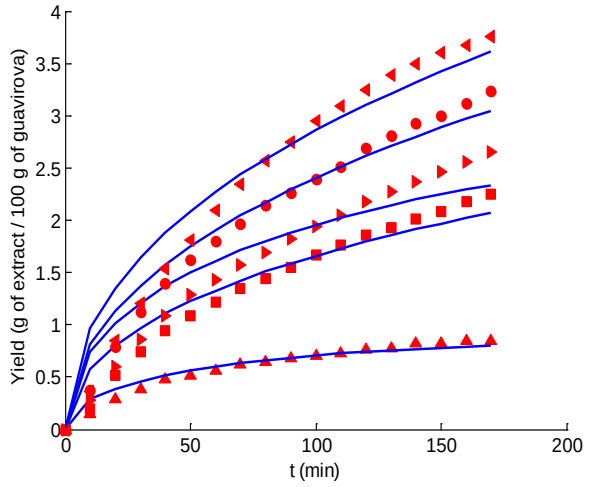

Figure 2. SFE of compounds from *Campomanesia xanthocarpa* fruits: comparison between the HSD model (——) and experimental data [6] at 313.15 K and 25 MPa (◀), 353.15 K and 25 MPa (●), 333.15 K and 20 MPa (▶), 313.15 K and 15.0 MPa (■), and 353.15 K and 15 MPa (▲)

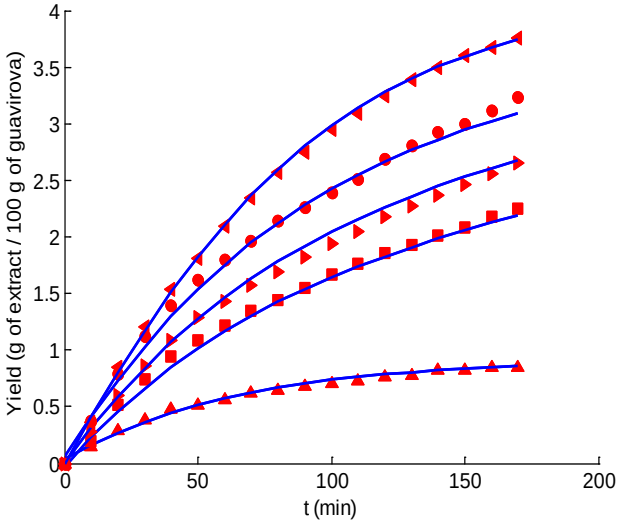

Figure 3. SFE of compounds from *Campomanesia xanthocarpa* fruits: comparison between the ANN model (——) and experimental data at 313.15 K and 25 MPa (◀), 353.15 K and 25 MPa (●), 333.15 K and 20 MPa (▶), 313.15 K and 15.0 MPa (■), and 353.15 K and 15 MPa (▲)

To compare the accuracy of both models precisely, their statistical performances are presented in Table 2. In spite of the fact that both models had approximately the same number of adjustable variables, 11 for ANN in comparison with 10 for HSD model, the produced errors for the ANN model were by far lower than those for the HSD model. Based on Table 2, the MSE for the ANN model changed from 0.0005, at 353.15 K and 15 MPa to just over 0.004 at 353.15 K and 25 MPa, whereas the MSE variation for the HSD model changed from just under 0.003 to approximately 0.068.

The MSE values of the ANN model for the training, test, and validation sets are shown in Tables 3. Although the MSE value of 0.0031 for the validation data set was higher than that of the training data set (0.0023), its test data set produced only a MSE value of 0.0016, which was approximately half of the corresponding value for the validation data set. It was reported in the literature that the ability of an ANN model for accurate prediction of test and validation data set is normally more valuable than the estimation ability for the training data [26]. Thus, low MSE values for the training, test, and validation sets of the current work signify an efficient ANN model.

Table 2. Comparison of the MSE values between the applied HSD model and the ANN model

Run	T (K)	P (MPa)	MSE	
			HSD	ANN
Exp. 1	353.15	15	0.0029	0.0005
Exp. 2	313.15	15	0.0243	0.0022
Exp. 3	333.15	20	0.0540	0.0039
Exp. 4	353.15	25	0.0293	0.0042
Exp. 5	313.15	25	0.0679	0.0009

Table 3. MSE values for the train, test, and validation sets of the constructed ANN model

Data Set	Number of Data	MSE
Training	36	0.0023
Test	27	0.0016
Validation	27	0.0031

3.2. Optimization

By employing ANN model, the extraction yields as a function of temperature and pressure are illustrated in Figure 4 at four distinct extraction times. It is clear that the overall trend of extraction efficiency for the smaller to medium pressures is almost the same all times. However, the trend for larger pressures is slightly different. In this region, although the extraction yield is a descending function of pressure at extraction times of 50 min and 70 min, it is pressure-independent at 120 min and especially at 170 min. Examining the figure at 170 min in more detail, the extraction yield rises from its lowest point at approximately 0.85 to a peak of just over 3.9 g of extract per 100 g of raw material. In contrast, temperature has a negative effect on the SFE performance and reduces it.

Figure 4 shows that the optimum operating conditions that maximize the extraction yield depend on the total extraction time. In other words, optimum operating conditions adopt different values depending on the total extraction time. This does not mean that the optimum temperature and pressure should be changed during the process, they are fixed values, and only these fixed values depend on the total extraction time. Thus, it is very interesting to determine the optimal pressure and temperature for various values of total extraction period. Based on the applied ANN model, the optimal operating conditions are shown in Figure 5. According to this figure, the optimum value of pressure increases gradually along with extraction time, but the

optimum value of temperature remains constant. For the small value of extraction time, the pressure of 17.9 MPa gives the best result, while the corresponding optimum value of temperature is 313.15 K. The optimum extraction yield at this operating condition is approximately 1.9 g of extract per 100 g of guavirova. By increasing the extraction time to 120 min and 170 min, the optimum pressure increases linearly to just over 18.5 MPa and approximately 18.8 MPa, respectively. Although the obtained optimum temperature in this paper (313 K) is the same as that obtained experimentally by Czaikoski et. al [6], there is a considerable difference between the obtained value for optimum pressure in this work, 17.9-18.8 MPa, compared to that in the literature, 25 MPa [6]. Even though Czaikoski et. al [6] obtained the best value of pressure experimentally, this does not mean that the result of the current study is incorrect. In fact, as Czaikoski et. al [6] performed at discrete combination of pressure and temperature, the operating condition 313.15 K and 25 MPa may not be the real optimum condition over the entire operating domain, it is just the best operating condition among the performed experiments. However, the optimum theoretical point in the current work was attained by continuously investigating the entire operating domains, 15 to 25 MPa for pressure and 313.15 to 353.15 K for temperature.

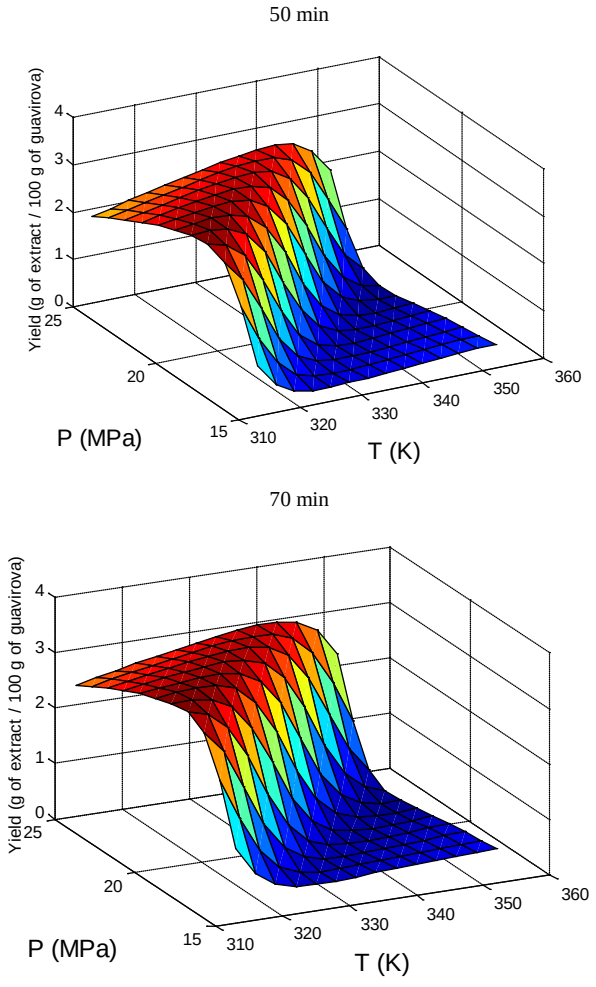

Figure 4. ANN surface plot for the SFE performance with respect to temperature and pressure at 50 min, 70 min, 120 min, and 170 min

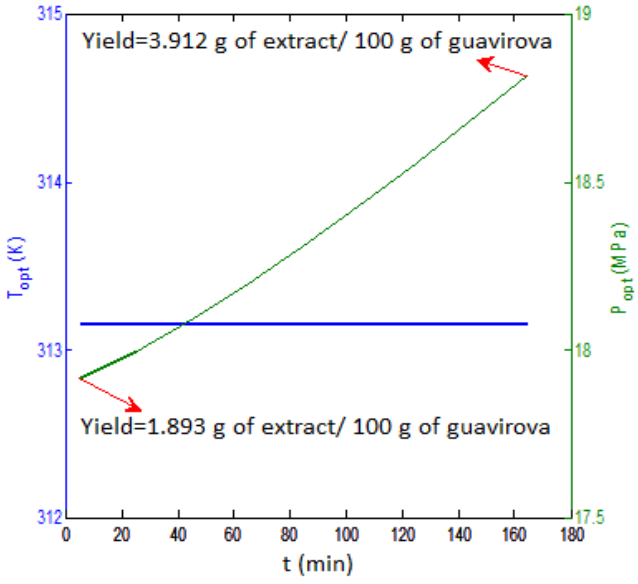

Figure 5. The optimum operating conditions at various values of the total extraction time

4. Conclusions

1) An ANN model with one hidden layer and two neurons was successfully employed to model the SFE of compounds from *Campomanesia xanthocarpa* fruits.
2) Although the HSD model produced acceptable results, its accuracy was far lower than that for the ANN model. For most of the experiments, the MSE of the HSD model was approximately ten times higher than that for the ANN model. The maximum value of MSE for the ANN model was 0.0042.
3) For the ANN model, the optimum value of temperature for maximizing the SFE yield was 313.15 K, which had been already reported in literature. In contrast, the ANN model revealed that the optimum value of pressure varies from 17.9 MPa for small extraction time to approximately 18.8 MPa for a higher extraction duration. Interestingly, it was reported in the literature that the temperature of 313.15 K and pressure of 25 MPa provided the highest SFE yield (3.9 extract per 100 g of raw material) among five distinct experiments. However, the results of the current study showed that it is also possible to achieve this amount of extraction yield by applying a smaller value of pressure in the range of 17.9 to 18.8 MPa.

REFERENCES

[1] Lorenzi H., Árvores brasileiras: manual de identificacão e cultivo de plantas arbóreas nativas do Brasil. 3rd Ed., Instituto Plantarum de Estudos da Flora, Nova Odessa, SP, 2009.

[2] Klafkea J. Z., Silva M. A. D., Panigasa T. F., Bellia K. C., Oliveira M. F. D., Barichello M. M., Rigo F. K., Rossato M. F., Santos A. R. S. D., Pizzolattie M. G., Ferreira J., and Viecilia P. R. N., Effects of Campomanesia xanthocarpa on biochemical, hema-tological and oxidative stress parameters in hypercholesterolemic patients. Journal of Ethnopharmacology 127 (2010) 299-305.

[3] Vinagre A. S., Ronnau A. D. S. R. O., Pereira S. F., Silveira L. U. D., Willand E. F., and Suyenaga E. S., Anti-diabetic effects of Campomanesia xanthocarpa (Berg) leaf decoc-tion. Brazilian Journal of Pharmaceutical Sciences 46 (2010) 169-177.

[4] Markman B.E.O., Bacchi E. M., and Kato E. T. M., Antiulcerogenic effects of Campo-manesia xanthocarpa. Journal of Ethnopharmacology 94 (2004) 55-57.

[5] Biavatti M. W., Farias C., Curtius F., Brasil L. M., Hort S., Schuster L., Leite S. N., and Prado S. R. T., Preliminary studies on Campomanesia xanthocarpa (Berg.) and Cuphea carthagenensis (Jacq.) J.F. Macbr. Aqueous extract: weight control andbiochemical parameters. Journal of Ethnopharmacology 93 (2004) 385-389.

[6] Czaikoski K., Mesomo M. C., Krüger R. L., Queiroga C. L., and Corazza M. L., Extraction of Campomanesia xanthocarpa fruit using supercritical CO_2 and bioactivity assessments. The Journal of Supercritical Fluids 98 (2015) 79-85.

[7] Fiori L., Lavelli V., Duba K. S., Harsha P. S. C. S., Mohamed H. B., and Guella G., Supercritical CO_2 extraction of oil from seeds of six grape cultivars: Modeling of mass transfer kinetics and evaluation of lipid profiles and tocol contents. The Journal of Supercritical Fluids 94 (2014) 71-80.

[8] Silva L. P. S., and Martínez J., Mathematical modeling of mass transfer in supercritical fluid extraction of oleoresin from red pepper. Journal of Food Engineering 133 (2014) 30-39.

[9] Scopel R., Falcão M. A., Lucas A. M., Almeida R. N., Gandolfi P. H. K., Cassel E., and Vargas R. M. F., Supercritical fluid extraction from Syzygium aromaticum buds: Phase equilibrium, mathematical modeling and antimicrobial activity. The Journal of Supercritical Fluids 92 (2014) 223-230.

[10] Zhang Y., Li H., Hou A., and Havel J., Artificial neural networks based on genetic input selection for quantification in overlapped capillary electrophoresis peaks. Talanta 65 (2005) 118-128.

[11] Izadifar M., and Abdolahi F., Comparison between neural network and mathematical modeling of supercritical CO_2 extraction of black pepper essential oil. The Journal of Supercritical Fluids 38 (2006) 37-43.

[12] Kuvendziev S., Lisichkov K., Zeković Z., and Marinkovski M., Artificial neural network modelling of supercritical fluid CO_2 extraction of polyunsaturated fatty acids from common carp (Cyprinus carpio L.) viscera. The Journal of Supercritical Fluids 92 (2014) 242-248.

[13] Ghoreishi S. M., and Heidari E., Extraction of Epigallocatechin-3-gallate from green tea via supercritical fluid technology: Neural network modeling and response surface optimization. The Journal of Supercritical Fluids 74 (2013) 128-136.

[14] Kamali M. J., and Mousavi M., 2008, Analytic, neural network, and hybrid modeling of supercritical extraction of α-pinene. The Journal of Supercritical Fluids, 47, 168-173.

[15] Khajeh M., Moghaddam M. G., and Shakeri M., 2012, Application of artificial neural network in predicting the extraction yield of essential oils of Diplotaenia cachrydifolia by supercritical fluid extraction. The Journal of Supercritical Fluids 69, 91-96.

[16] Fatehi M. R., Raeissi S., and Mowla D., An artificial neural network to calculate pure ionic liquid densities without the need for any experimental data. The Journal of Supercritical Fluids 95 (2014) 60-67.

[17] Vaferi B., Karimi M., Azizi M., and Esmaeili H., Comparison between the artificial neural network, SAFT and PRSV approach in obtaining the solubility of solid aromatic compounds in supercritical carbon dioxide. The Journal of Supercritical Fluids 77 (2013) 44-51.

[18] Lashkarbolooki M., Shafipour Z. S., Hezave A. Z., and Farmani H., Use of artificial neural networks for prediction of phase equilibria in the binary system containing carbon dioxide. The Journal of Supercritical Fluids 75 (2013) 144-151.

[19] Zhang Y., and Pan B., Modeling batch and column phosphate removal by hydrated ferric oxide-based nanocomposite using

response surface methodology and artificial neural network. Chemical Engineering Journal 249 (2014) 111-120.

[20] Olden J. D., and Jackson D. A., Illuminating the ‘‘black box’’: a randomization approach for understanding variable contributions in artificial neural networks. Ecological Modelling 154 (2002) 135–150.

[21] Crank J., The mathematics of diffusion 2 ed. ed., Clarendon Press, Oxford, UK, 1975.

[22] Heidari E., and Ghoreishi S. M., Prediction of supercritical extraction recovery of EGCG using hybrid of Adaptive Neuro-Fuzzy Inference System and mathematical model. The Journal of Supercritical Fluids 82 (2013) 158-167.

[23] Chen W., Lu X., Yao C., Zhu G., and Xu Z., An efficient approach based on bi-sensitivity analysis and genetic algorithm for calibration of activated sludge models. Chemical Engineering Journal 259 (2015) 845-853.

[24] Lin S., Luan F., Han Z., Lü X., Zhou X., and Liu W., Genetic Algorithm Based on Duality Principle for Bilevel Programming Problem in Steel-making Production. Chinese Journal of Chemical Engineering 22 (2014) 742-747.

[25] Ge Y., Li S., and Qu K., A Novel Empirical Equation for Relative Permeability in Low Permeability Reservoirs. Chinese Journal of Chemical Engineering 22 (2014) 1274-1278.

[26] Nay M. E. G., and Yildirim R., Analysis of selective CO oxidation over promoted Pt/Al_2O_3 catalysts using modular neural networks: Combining preparation and operational variables. Applied Catalysis A: General 377 (2010) 174–180.